Molecular Biology of the Cell
Vol. 14, 1545–1557, April 2003

Morphology and Dynamics of Clathrin/GGA1-coated Carriers Budding from the *Trans*-Golgi Network[V]

Rosa Puertollano,* Nicole N. van der Wel,† Lois E. Greene,‡ Evan Eisenberg,‡ Peter J. Peters,† and Juan S. Bonifacino*§

*Cell Biology and Metabolism Branch, National Institute of Child Health and Human Development and Laboratory of Cell Biology, National Heart, Lung, and Blood Institute, National Institutes of Health, Bethesda, Maryland 20892; and †Division of Tumor Biology, The Netherlands Cancer Institute, Amsterdam, The Netherlands

Submitted July 15, 2002; Revised October 22, 2002; Accepted December 4, 2002
Monitoring Editor: Suzanne R. Pfeffer

Sorting of transmembrane proteins and their ligands at various compartments of the endocytic and secretory pathways is mediated by selective incorporation into clathrin-coated intermediates. Previous morphological and biochemical studies have shown that these clathrin-coated intermediates consist of spherical vesicles with a diameter of 60–100 nm. Herein, we report the use of fluorescent imaging of live cells to demonstrate the existence of a different type of transport intermediate containing associated clathrin coats. Clathrin and the adaptors GGA1 and adaptor protein-1, labeled with different spectral variants of the green fluorescent protein, are shown to colocalize to the *trans*-Golgi network and to a population of vesicles and tubules budding from it. These intermediates are highly pleiomorphic and move toward the peripheral cytoplasm for distances of up to 10 μm with average speeds of $\sim$1 μm/s. The labeled clathrin and GGA1 cycle on and off membranes with half-times of 10–20 s, independently of vesicle budding. Our observations indicate the existence of a novel type of *trans*-Golgi network-derived carriers containing associated clathrin, GGA1 and adaptor protein-1 that are larger than conventional clathrin-coated vesicles, and that undergo long-range translocation in the cytoplasm before losing their coats.

INTRODUCTION

Clathrin coats associated with the cytosolic face of membranes mediate the sorting of transmembrane proteins and their bound ligands at the plasma membrane, the *trans*-Golgi network (TGN) and endosomes (Kirchhausen, 2000; Brodsky *et al.*, 2001). The major building blocks of clathrin coats are clathrin triskelia composed of three heavy chains and three light chains (a or b isoforms), which assemble into polyhedral lattices. At each intracellular location, clathrin coats contain a characteristic set of heterotetrameric adaptor protein (AP) complexes that mediate both attachment of the clathrin lattices to membranes and concentration of specific transmembrane proteins. The AP-2 complex plays such roles at the plasma membrane, whereas the AP-1 complex does so at the TGN and/or endosomes (Kirchhausen, 2000; Brodsky *et al.*, 2001; Robinson and Bonifacino, 2001). Recently, a family of monomeric proteins termed GGAs (i.e., GGA1, GGA2, and GGA3 in humans) has also been shown to promote recruitment of clathrin and sorting of transmembrane proteins at the TGN (Robinson and Bonifacino, 2001; Boman, 2001). In particular, the GGAs have been implicated in the sorting the cation-dependent and cation-independent mannose 6-phosphate receptors (CD- and CI-MPRs, respectively) from the TGN to the endosomal-lysosomal system (Puertollano *et al.*, 2001a; Takatsu *et al.*, 2001; Zhu *et al.*, 2001). This sorting is mediated by interaction of the amino-terminal VHS domain of the GGAs and acidic-cluster–dileucine sorting signals present in the cytoplasmic domains of the MPRs (Puertollano *et al.*, 2001a; Takatsu *et al.*, 2001; Zhu *et al.*, 2001). The VHS domain of the GGAs has also been shown to interact with acidic-cluster–dileucine signals in the cytoplasmic domains of other transmembrane proteins such as sortilin (Nielsen *et al.*, 2001), the low-density lipoprotein receptor-related protein 3 (Takatsu *et al.*, 2001), and β-secretase (He *et al.*, 2002), all of which may also cycle between the TGN and endosomes.

Despite recent advances in the elucidation of the role of the GGAs in protein sorting, many outstanding issues remain concerning 1) whether the GGAs colocalize with clathrin and AP-1 on transport intermediates budding from the

Article published online ahead of print. Mol. Biol. Cell 10.1091/mbc.02–07–0109. Article and publication date are at www.molbiolcell.org/cgi/doi/10.1091/mbc.02–07–0109.

[V] Online version of this article contains video material for some figures. Online version available at www.molbiolcell.org.

§ Corresponding author. E-mail address: juan@helix.nih.gov.

TGN, 2) the morphology of these GGA-containing intermediates, 3) the intracellular destination of these carriers, and 4) the dynamics of GGA cycling on and off TGN membranes in vivo. These issues have recently become amenable to analysis through the use of fluorescence imaging technologies on live cells. The dynamics of plasma membrane clathrin-coated pits, for example, have been examined using clathrin constructs tagged with variants of the green fluorescent protein (GFP) (Gaidarov *et al.*, 1999; Damer and O'Halloran, 2000; Wu *et al.*, 2001). This approach revealed that clathrin-coated vesicles (CCVs) emanate repeatedly from the same sites, suggesting the existence of "hot-spots" for CCV formation from the plasma membrane (Gaidarov *et al.*, 1999). The same approach was used to demonstrate a rapid ($t_{1/2}$ ~16 s), ATP-dependent exchange of clathrin triskelia on plasma membrane coated pits, which may allow remodeling of the coat as the membrane invaginates (Wu *et al.*, 2001). Strikingly, clathrin exchange on the pits occurs even when endocytosis is blocked (Wu *et al.*, 2001), indicating that the coats are not static assemblies and that uncoating does not require vesicle detachment from the membrane. To date, the characteristics of protein coats associated with the TGN in living cells remain to be similarly examined.

Herein, we report the results of a study on the morphology and dynamics of GGA1-, AP-1-, and clathrin-coated structures at the TGN in vivo. By using GGA1, the γ1 subunit of AP-1, and clathrin light chain b isoform labeled with different spectral variants of GFP, we show that all of these coat proteins colocalize to the TGN and to a population of vesicular-tubular carriers budding from the TGN. Surprisingly, these carriers are pleiomorphic and apparently larger than conventional CCVs. They move centrifugally for distances of up to 10 μm and with average speeds of 1 μm/s. The fluorescently labeled clathrin and GGA1 constructs cycle on and off membranes with $t_{1/2}$ of 10–20 s. This cycling is not dependent on budding from the TGN, suggesting that assembly and disassembly of the coats can be functionally uncoupled from vesicle budding. These results suggest the existence of a novel type of TGN-derived carriers containing associated clathrin that are larger and more dynamic than conventional CCVs, and that undergo long-range translocation in the cytoplasm before losing their coat.

MATERIALS AND METHODS

Recombinant DNA Procedures and Antibodies

A cDNA encoding full-length human GGA1 was cloned into the *Sal*I and *Bam*HI sites of the pEGFP-C1, pEYFP-C1, and pECFP-C1 vectors (BD Biosciences Clontech, Palo Alto, CA). Clathrin light chain b was amplified from human placenta Quick-Clone cDNA (BD Biosciences Clontech) and cloned into the pEYFP-C2 vector via *Eco*RI and *Sal*I sites. Plasmids encoding cyan fluorescent protein (CFP)-vesicular stomatitis virus G (VSV-G) (ts045 mutant) and CFP-galactosyl transferase were the kind gift of Jennifer Lippincott-Schwartz (National Institute of Child Health and Human Development). The cloning of the Myc-epitope-tagged GGA1 and CD-MPR-CFP was described previously (Dell'Angelica *et al.*, 2000; Puertollano *et al.*, 2001a).

The following commercial antibodies were used: mouse monoclonal and rabbit polyclonal anti-myc antibodies (9E10; Covance, Princeton, NJ), mouse monoclonal antibody to γ1-adaptin (100/3, Sigma-Aldrich, St. Louis, MO), and mouse monoclonal antibody to clathrin (CHC; Transduction Laboratories, Lexington, KY). The preparation of rabbit polyclonal antibody to AP-3 (β3C1) has been described in a previous report (Dell'Angelica *et al.*, 2000). A polyclonal antibody to GGA1 was the kind gift of Margaret S. Robinson (University of Cambridge, Cambridge, United Kingdom).

Immunofluorescence Microscopy

Nonpolarized Madin-Darby canine kidney (MDCK) cells were grown on coverslips and fixed in methanol/acetone (1:1, vol/vol) for 10 min at −20°C and subsequently air-dried. Incubation with primary antibodies diluted in phosphate-buffered saline (PBS), 0.1% (wt/vol) saponin, 0.1% bovine serum albumin, was carried out for 1 h at room temperature. Unbound antibodies were removed by rinsing with phosphate-buffered saline for 5 min, and cells were subsequently incubated with secondary antibodies (Cy3-conjugated donkey anti-rabbit Ig and Alexa 448–conjugated donkey anti-mouse Ig) diluted in PBS, 0.1% (wt/vol) saponin, 0.1% bovine serum albumin, for 30–60 min at room temperature. After a final rinse with PBS, coverslips were mounted onto glass slides with Fluoromount G (Southern Biotechnology Associates, Birmingham, AL). Fluorescence images were acquired on an LSM 410 or LSM 510 confocal microscope (Carl Zeiss, Thornwood, NY).

Immunoelectron Microscopy

Cryogold immunoelectron microscopy of monocyte-derived dendritic cells and stably transfected MDCK cells was performed as described previously (Porcelli *et al.*, 1992; Peters, 1998)

Fluorescent Imaging of Living Cells

MDCK cells were grown on LabTek chambers (Nalge Nunc, Naperville, IL), transfected with different constructs tagged with GFP spectral variants by using FuGENE 6 (Roche Diagnostics, Indianapolis, IN), and transferred into culture medium buffered with 25 mM HEPES/KOH pH 7.4. Experiments were performed using an inverted confocal laser scanning microscope (LSM 510; Carl Zeiss) equipped with a stage heated to 37°C. argon, HeNe, and krypton lasers; and a 63× 1.4 numerical aperture objective. Yellow fluorescent protein (YFP) and CFP fluorescence were visualized using excitation filters at 514 and 413 nm and emission filters at 530 and 515–430 nm, respectively, whereas GFP was excited with a 488-nm filter and imaged through a 515- to 545-nm emission filter. When indicated, endosomes were loaded with rhodamine-conjugated human serum albumin or rhodamine-conjugated transferrin (Molecular Probes, Eugene, OR), which were imaged using a 543-nm laser. Cells expressing CFP-VSV-G (ts045 mutant) were cultured at 40°C for 24 h, shifted to 20°C for 1 h, and then to 32°C before visualization. Images were recorded every 3 or 6 s. To estimate the size of GGA1-coated intermediaries, MDCK cells expressing YFP-GGA1 were incubated with medium containing yellow-green fluorescent beads (FluoSpheres carboxylate-modified microspheres, 2.0 μm; Molecular Probes) and analyzed by time-lapse confocal microscopy as described previously. Data were processed to QuickTime format in Adobe Premiere 5.0.

Photobleaching was performed at high laser power (100% power, 100% transmission). Recovery was followed by scanning the whole cell at lower power (40%) and attenuated transmission (3%) at intervals from 5 s to 5 min. A nearby background region of equal area was similarly measured and subtracted. Background pixel values were <20% of the average intensity of these structures. Fluorescence intensity was normalized to the first time point.

RESULTS

Distribution of Coat Proteins Associated with TGN in MDCK Cells

We chose to perform our imaging studies on nonpolarized MDCK epithelial cells because they 1) are large and flat, 2)

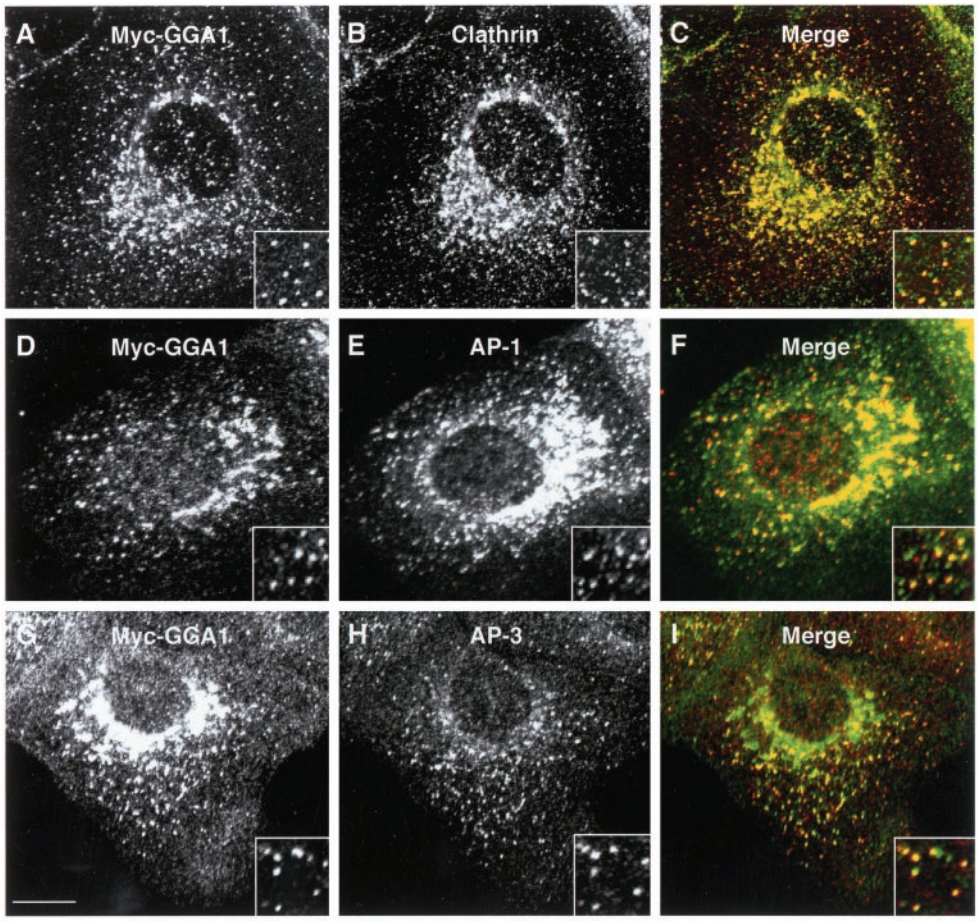

Figure 1. Intracellular distribution of Myc-GGA1 in MDCK cells analyzed by immunofluorescence microscopy. MDCK cells stably expressing Myc-GGA1 were fixed, permeabilized, and double labeled by incubation with antibodies to GGA1 (A, red channel), the Myc epitope (D, red channel; G, green channel), clathrin (B, green channel), the γ1-adaptin subunit of AP-1 (E, green channel), and the β3A subunit of the AP-3 complex (H, red channel), as indicated in the figure, followed by the corresponding fluorescently conjugated secondary antibodies. Stained cells were examined by confocal fluorescence microscopy. Merging the images in the red and green channels generated the third picture on each row (C, F, and I); yellow indicates overlapping localization. Insets show twofold-magnified views of peripheral cytoplasmic regions. Bar, 10 μm.

have an extensive TGN, and 3) yield low-to-moderate expression of constructs driven from the human cytomegalovirus promoter, as is the case for the plasmid vectors used herein. The use of MDCK cells, however, necessitated a reexamination of the distribution of various coat proteins associated with the TGN, as previously established for other cell lines. We started by performing immunofluorescence microscopy of MDCK cells stably transfected with a Myc-tagged GGA1 construct (Myc-GGA1). Immunoblot analyses with an antibody to GGA1 revealed that the expression levels of Myc-GGA1 were four- to fivefold higher than those of endogenous GGA1 (our unpublished data). Consistent with previous findings in other cell lines (Hirst *et al.*, 2001; Puertollano *et al.*, 2001b), we observed extensive colocalization of Myc-GGA1 with clathrin in the area of the TGN (Figure 1, A–C). We also observed considerable overlap of Myc-GGA1 and AP-1 staining at the TGN (Figure 1, D–F). Outside the TGN, Myc-GGA1, AP-1, and clathrin displayed various degrees of colocalization to cytoplasmic structures having apparent diameters of ~400 nm (Figure 1, insets). Quantification of these results showed that almost 100% of all resolvable GGA1-containing foci colocalized with clathrin (148 foci counted), whereas 40% colocalized with AP-1 (110 foci counted). Another AP complex, AP-3, was more peripherally distributed than either GGA1 or AP-1 and therefore exhibited substantially less colocalization with Myc-GGA1 in the area of the TGN (Figure 1, G–I). Some peripheral foci, however, seemed to contain both AP-3 and Myc-GGA1 (Figure 1, G–I, inset).

Immunoelectron microscopy of monocyte-derived dendritic cells, in which endogenous GGA1 can be more easily detected, revealed localization of endogenous GGA1 to coated buds with diameters of 60–130 nm in the area of the TGN (Figure 2A), as well as in the peripheral cytoplasm (our unpublished data). A similar localization was observed for Myc-GGA1 in stably transfected MDCK cells (Figure 2, B–D). Many coated buds were found to contain both Myc-GGA1 and clathrin (Figure 2B, open arrowheads). We also observed partial colocalization of Myc-GGA1 and AP-1 on coated buds with diameters of 60–130 nm at both the TGN (Figure 2, C–D, open arrowheads) and the cell periphery (Figure 2D, open arrowheads). However, some individual buds contained gold particles labeling only Myc-GGA1 or AP-1 (Figure 2, C and D). We detected some gold labeling for all of these coat proteins in the cytosol, consistent with the fact that they cycle between membranes and the cytosol. Buds containing these coat proteins often occurred in mixed clusters, which might correspond to the larger peripheral structures observed by fluorescence microscopy.

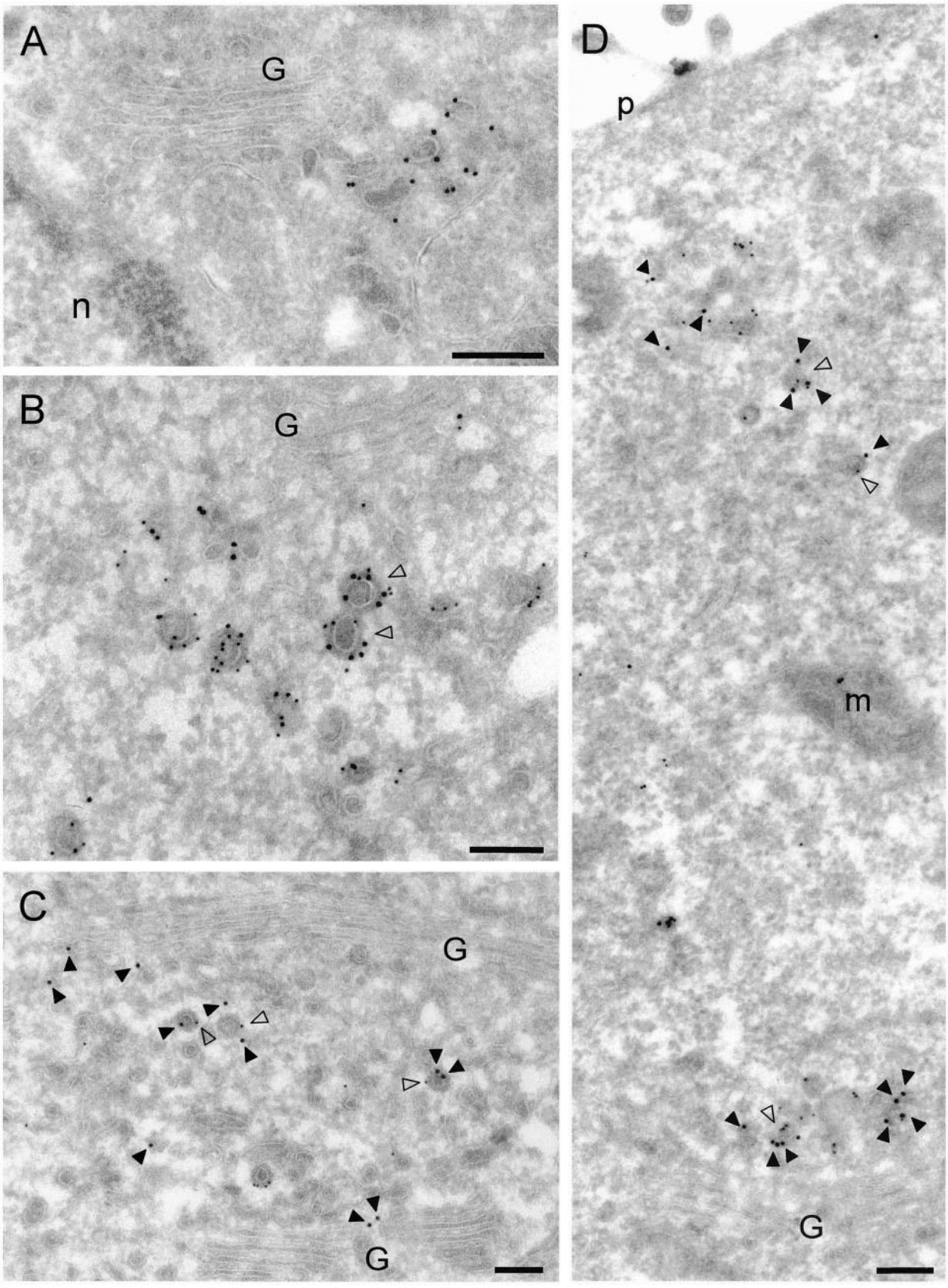

Figure 2.

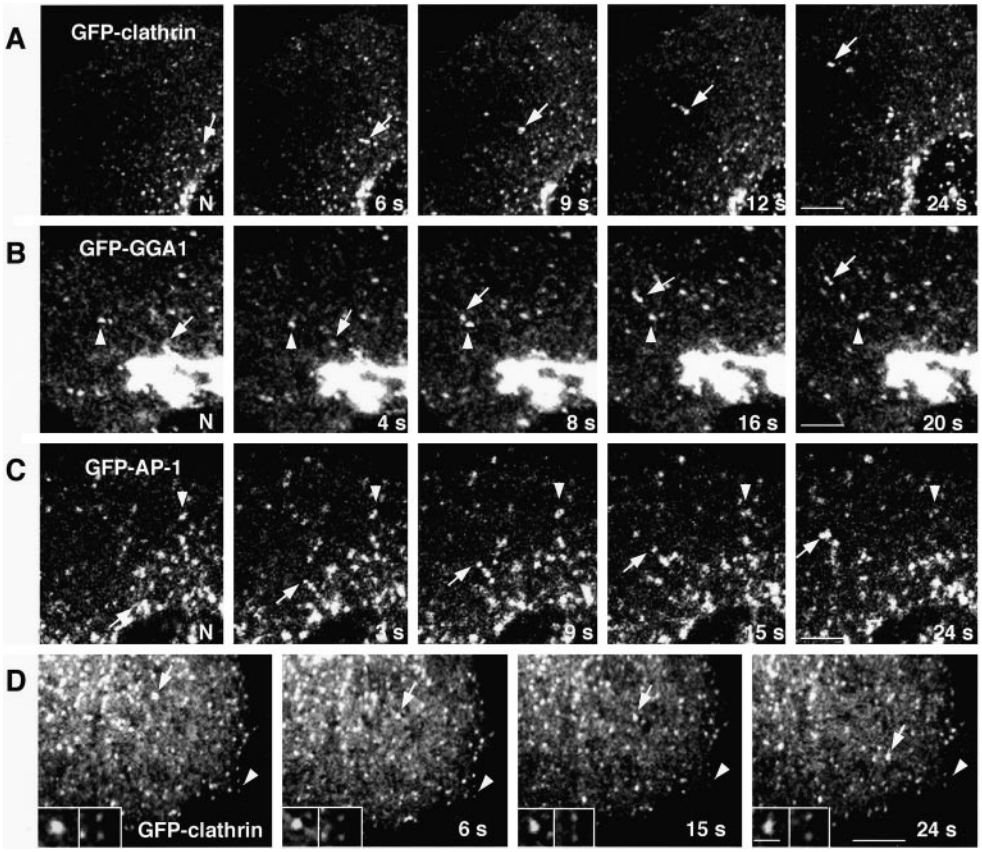

Figure 3. Characterization of TGN-derived carriers containing clathrin, GGA1, and AP-1. MDCK cells were grown on LabTek chambers and transiently transfected with constructs encoding GFP-clathrin light chain b (A and D), GFP-GGA1 (B), or GFP-γ1-adaptin (GFP-AP-1; C). At 15 h after transfection, cells expressing moderate levels of the fluorescent proteins were analyzed by time-lapse microscopy and images acquired at the indicated intervals. Insets in D show twofold-magnified comparisons of clathrin-containing carriers budding from the TGN with clathrin-coated pits at the plasma membrane. Arrows point to pleiomorphic carriers budding from the TGN and moving toward the cell periphery, whereas arrowheads indicate immobile structures. N, nucleus. Bars, 5 μm (A–C), 4 μm (D), 1 μm (D insets). QuickTime videos of the experiments shown in A, B, and C can be seen in Supplemental Materials (videos 1, 2, and 3, respectively).

Characteristics of Coated Carriers Budding from TGN

To examine the morphology and dynamics of coated carrier vesicles budding from the TGN, we constructed plasmids encoding various spectral variants of GFP attached to clathrin light chain b isoform, GGA1 and the γ1-adaptin subunit of AP-1. These proteins were expressed by transfection into MDCK cells. At low-to-moderate levels of expression, all three GFP-tagged proteins localized to both juxtanuclear and peripheral structures (Figure 3, A–C), similar to those shown in Figure 1. Time-lapse confocal microscopy of live cells expressing each of these GFP-tagged constructs revealed that some of the peripheral foci were relatively static (arrowheads), whereas others moved rapidly from the TGN toward the peripheral cytoplasm (arrows) (Figure 3, A–C). The structures emanating from the TGN were relatively large (360- to 380-nm average diameters; Table 1) in comparison with plasma membrane clathrin-coated pits (Gaidarov *et al.*, 1999; Wu *et al.*, 2001). This difference could be readily appreciated in fields where the larger TGN-derived,

Figure 2 (facing page. Immunoelectron microscopy localization of GGA1, Myc-GGA1, clathrin and AP-1. (A) Localization of endogenous GGA1 in monocyte-derived dendritic cells was analyzed by cryoimmunogold electron microscopy using antibodies to GGA1 (10-nm gold). (B–D) MDCK cells stably expressing Myc-GGA1 were analyzed by cryoimmunogold electron microscopy using antibodies to the Myc epitope (15-nm gold) and clathrin (10-nm gold) (B), GGA1 (15-nm gold) and the γ1 subunit of AP-1 (10-nm gold) (C and D). Open arrowheads in B indicate coated buds containing both Myc-GGA1 and clathrin, whereas closed arrowheads point to 15-nm gold particles marking the location of Myc-GGA1. Open arrowheads in C and D point to coated buds containing both Myc-GGA1 (or GGA1) and AP-1, whereas closed arrowheads point to 15-nm gold particles marking the location of Myc-GGA1 (or GGA1). G, Golgi complex; n, nucleus; p, plasma membrane; m, mitochondrion. Bars, 200 nm.

Table 1. Quantification of the size of foci containing fluorescently labeled clathrin and GGA1

GFP fusion proteins	Size (nm)	n
GFP-clathrin (moving from the TGN area)	360 ± 60	30
GFP-clathrin (plasma membrane)	180 ± 40	30
GFP-GGA1 (moving from the TGN area)	380 ± 50	24

MDCK cells expressing GFP-fusion proteins were analyzed for the size of moving foci emanating from the TGN (GFP-clathrin and GFP-GGA1) and at plasma membrane (GFP-clathrin). Sizes were estimated from fluorescence microscopy images. Size values are the mean ± SD of the number of determinations (n) indicated in the Table.

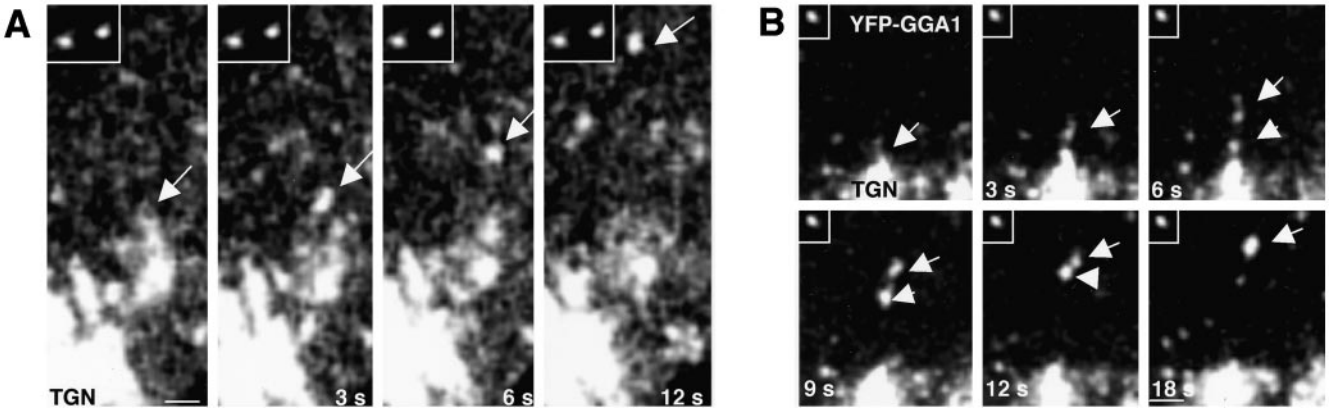

Figure 4. Comparison of the size of GGA1-coated intermediaries to that of fluorescent beads. MDCK cells expressing YFP-GGA1 were incubated with 0.2-μm-diameter fluorescent beads before analysis by time-lapse confocal microscopy. Arrow in A points to a YFP-GGA1–containing intermediate moving from the TGN toward the cell periphery. Notice that this carrier seems larger (~0.35 μm) than the beads shown in the inset (~0.2 μm), even though these structures have similar fluorescent intensities (37.7 and 38.6 arbitrary units, respectively). In some cases, large intermediates seem to arise from clustering of smaller vesicles, as shown in B (fluorescent bead is shown in the inset). Bars, 0.5 μm (A), 1 μm (B).

clathrin-coated intermediates moved in relation to smaller, less mobile clathrin-coated pits at the cell edges (Figure 3D, size comparison shown in the insets). In addition, the intermediates seemed larger than 200-nm-diameter fluorescent beads of similar brightness added to the cell cultures before imaging (Figure 4A, compare fluorescent beads in the insets with moving intermediate indicated by arrow).

The TGN-derived intermediates decorated with any of the three GFP-fusion proteins were pleiomorphic. Most were spheroidal or ellipsoidal. Some detached from the TGN as single vesicles, whereas others pulled off in groups resembling beads on a string (e.g., Figures 3C, 6A, and 7, A and B). They often changed shapes and some even divided during transport (Figure 5B, arrow between 6 and 9 s). Others joined or fused during transport, generating structures that were bigger and brighter than the original vesicles (Figure 4B).

The TGN-derived intermediates moved centrifugally with average speeds of ~1 μm/s. Their trajectories were quasilinear, as if they were tethered to a system of radial tracks. Treatment with the microtubule-depolymerizing agent, nocodazole, abolished the long-range translocation of the TGN-derived intermediates (our unpublished data), suggesting that movement occurred along microtubules.

Coexpression of combinations of coat proteins, each tagged with a different GFP variant, allowed us to analyze for their presence on the same coated intermediates. We observed that most TGN-derived intermediates contained both clathrin and GGA1 (an example is shown in Figure 5A). We could also observe budding of intermediates that contained both GGA1 and AP-1 (Figure 5B).

As previously shown (Puertollano *et al.*, 2001a), tubules and vesicles carrying the CD-MPR from the TGN almost always exhibited associated GGA1. In the example shown in Figure 6A, a string of GGA1-containing structures can be seen decorating in discontinuous manner a CD-MPR-carrying tubule. We occasionally saw endosomal recycling tubules labeled with internalized rhodamine-transferrin pulling off the juxtanuclear area of the cell, but these almost never contained associated GGA1 (Figure 6B). Although GGA1- and AP-1–containing intermediates detached and moved away from the TGN, the Golgi resident enzyme galactosyl transferase stayed behind in the Golgi complex (Figure 7, A and B). GGA1-containing intermediates were distinct from post-Golgi carriers (i.e., PGCs; Hirschberg *et al.*, 1998; Polishchuk *et al.*, 2000) that transport the VSV-G protein to the plasma membrane (Figure 7C). These observations illustrate the occurrence of protein sorting at the TGN by generation of distinct types of vesicular carriers.

Interaction of GGA1-containing Carriers with Endosomes

On arrival at the cell periphery, the fluorescent signal of most TGN-derived, GGA1-containing carriers was lost, perhaps due to uncoating or movement outside the plane of focus. This prevented us from establishing the final destination of these carriers. Some GGA1-containing structures, however, were found to interact with endosomes labeled by internalization of rhodamine-albumin for 15 min. Figure 8 shows an example of such interactions. In this example, a GFP-GGA1–coated carrier (green) and a rhodamine-albumin–containing endosome (red) converge to form a single hybrid organelle (yellow). The two markers remain associated with the same structure and move together for 51 s, although at times they seem segregated to different domains of the hybrid organelle. This structure eventually undergoes uneven fission into a vesicle that contains both GGA1 and albumin and another vesicle that contains only GGA1. The latter finally disappears, likely due to uncoating. We have observed variations on this phenomenon. Sometimes the GFP-GGA1 fluorescence is quickly lost after the two vesicles merge. Other times the GGA1- and albumin–containing vesicles interact transiently and then part ways, reminiscent of "kiss-and-run" interactions (Storrie and Desjardins, 1996). We interpret that these events represent the transfer of cargo from the TGN-derived carriers to the endosomal system.

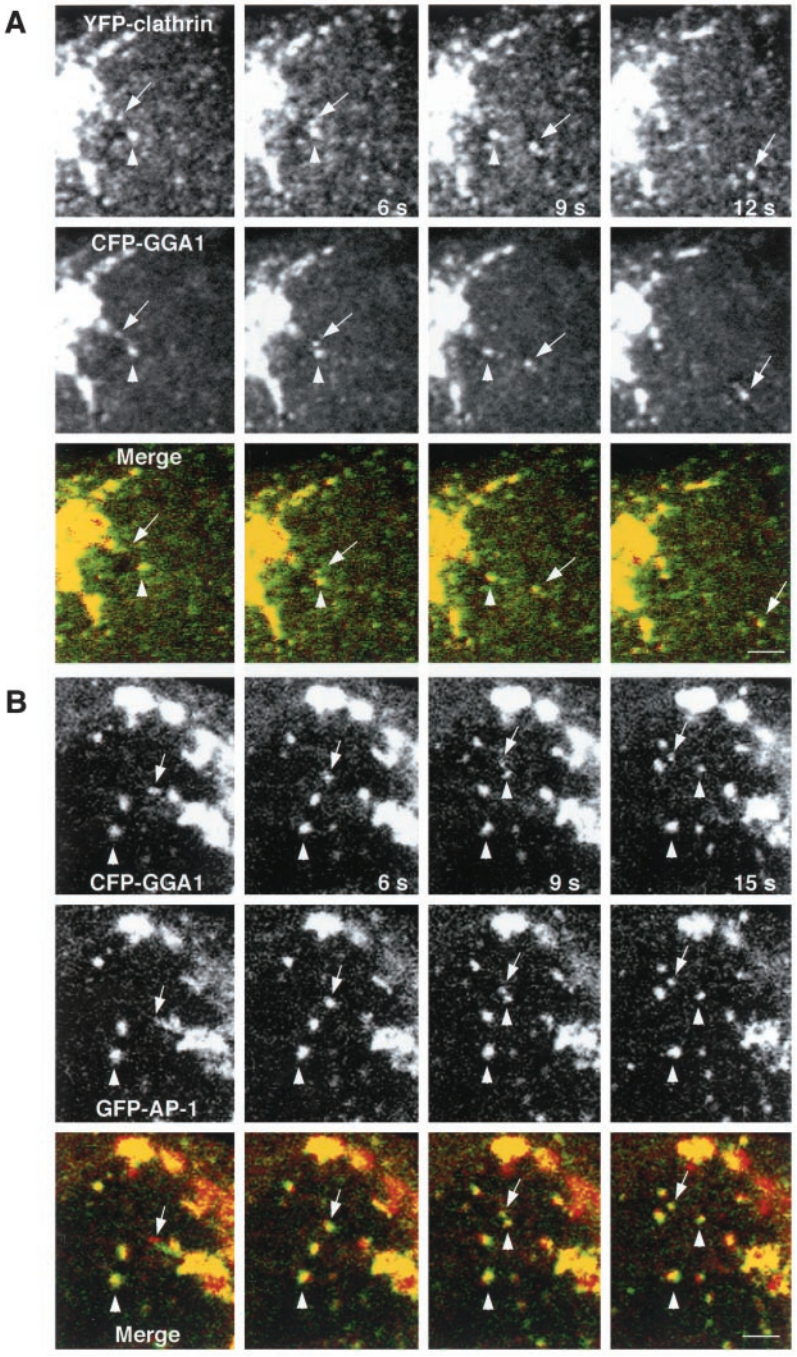

Figure 5. Presence of clathrin and AP-1 on GGA1-containing carriers. MDCK cells were simultaneously transfected with constructs encoding YFP-clathrin and CFP-GGA1 (A) or GFP-γ1 (GFP-AP-1) and CFP-GGA1 (B). Confocal microscopy images were acquired every 3 s. Arrows indicate vesicular carriers budding from the TGN, whereas arrowheads point to immobile structures. The yellow color in the merged images indicates colocalization between clathrin and GGA1 (A) or GGA1 and AP-1 (B). Bars, 2 μm.

Dynamics of Clathrin and GGA1 Coats

The ability to visualize fluorescently tagged clathrin and GGA1 in association with the TGN allowed us to examine the rates of exchange of these proteins between membranes and the cytosol by using the technique of fluorescence recovery after photobleaching (Jacobson *et al.*, 1976). This was performed by photobleaching a region of the TGN and quantifying the time course of fluorescence recovery in that region. We found that both GFP-clathrin (Figure 9A) and GFP-GGA1 fluorescence (Figure 9B) recovered with exponential kinetics and $t_{1/2}$ of ~20 and 10 s, respectively (Figure 9D). These rates were within the range previously reported for clathrin at the plasma membrane (Wu *et al.*, 2001) and COPI on the Golgi complex (Presley *et al.*, 2002). Hence, the association of all of these proteins' coats with membranes is a highly dynamic process. The recovery seemed to occur on the same structures that were photobleached (Figure 9C, arrows).

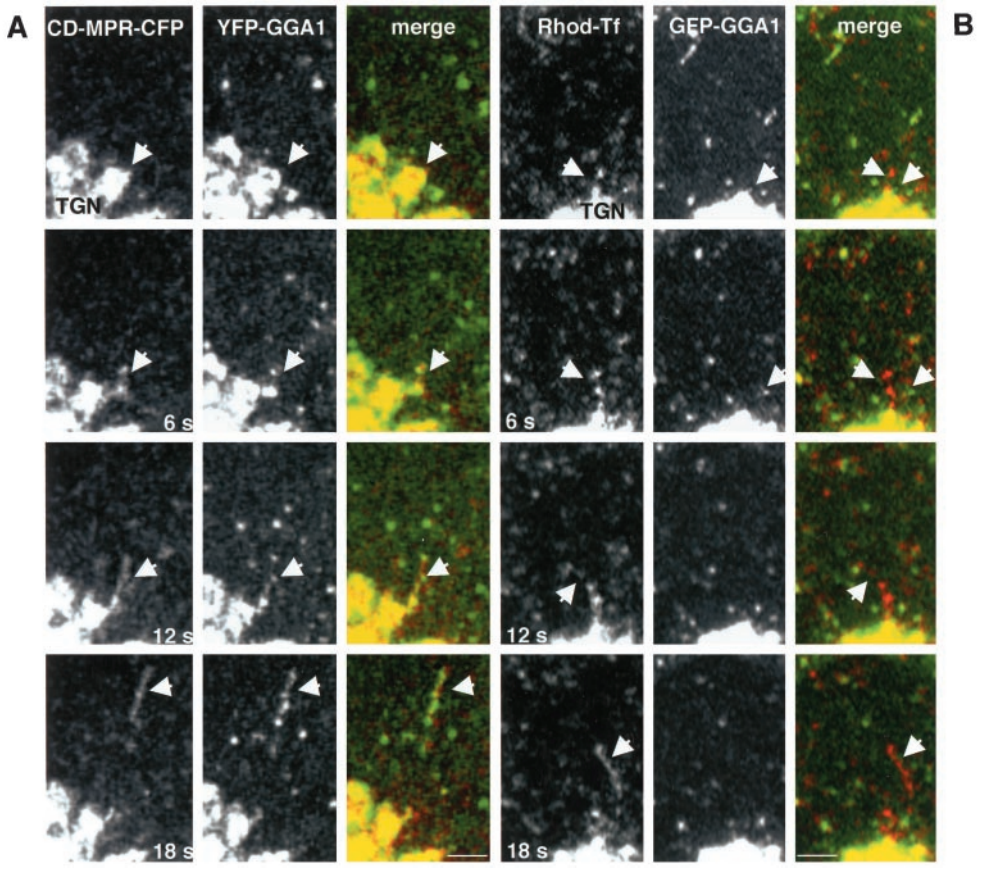

Figure 6. Cargo specificity of GGA1-containing intermediates. (A) Confocal microscopy imaging of live MDCK cells coexpressing CD-MPR-CFP and YFP-GGA1. Images were collected at 6-s intervals. Arrows indicate the formation and detachment of long tubular structures containing CD-MPR-CFP from the TGN. Notice that YFP-GGA1 associates with those tubular structures in a discontinuous pattern. (B) MDCK cells expressing GFP-GGA1 were incubated with rhodamine-transferrin for 20 min to load recycling endosomes and then examined by video microscopy. Images show that transferrin-containing intermediates in transit from the juxtanuclear area of the cell are devoid of GFP-GGA1. Bars, 3 μm.

To assess whether membrane binding and release of GFP-clathrin and GFP-GGA1 were coupled to vesicle budding from the TGN, we examined the effect of lowering the temperature to 20°C, a manipulation that blocks protein export from the TGN to various compartments (Griffiths *et al.*, 1985; Xu and Shields, 1993; Wacker *et al.*, 1997), including those of the endosomal-lysosomal system (Nishimura *et al.*, 1990). We observed that budding of clathrin- and GGA1-containing intermediates completely ceased at this temperature (our unpublished data). Strikingly, the majority of GGA1 and clathrin fluorescence on the TGN still recovered at 20°C, albeit more slowly (Figure 9D). These results indicate that GGA1 and clathrin continue to undergo cycling on and off the TGN membrane even when vesicle budding from the TGN is inhibited. Thus, the association and dissociation of these TGN coat proteins with membranes is not obligatorily coupled to vesicle formation and budding.

DISCUSSION

The results presented herein demonstrate that clathrin, GGA1, and AP-1 are associated with a population of vesicular-tubular carriers budding from the TGN. These carriers look larger and more pleiomorphic than conventional CCVs. After detaching from the TGN, the carriers move along microtubules for distances of up to ~10 μm toward the peripheral cytoplasm. The signal of the fluorescently labeled coat proteins associated with the carriers disappears at different times after reaching the cell periphery, probably due to uncoating. Some coated carriers, however, persist and can be seen engaging in fusion or kiss-and-run interactions with peripheral endosomes before they lose their coat. Thus, it is likely that a function of these coated carriers is to move cargo between the TGN and peripheral endosomes.

A cargo molecule transported by these intermediates is the CD-MPR, which interacts via acidic-cluster–dileucine signals with the VHS domain of the GGAs (Puertollano *et al.*, 2001a; Takatsu *et al.*, 2001; Doray *et al.*, 2002a). Indeed, we observed that the CD-MPR leaves the TGN on vesicular-tubular structures decorated with GGA1. Other transmembrane proteins such as the CI-MPR (Puertollano *et al.*, 2001a; Takatsu *et al.*, 2001; Zhu *et al.*, 2001), sortilin (Nielsen *et al.*, 2001), the low-density lipoprotein-related protein 3 (Takatsu *et al.*, 2001), and β-secretase (He *et al.*, 2002), also have acidic-cluster–dileucine signals that interact with the GGAs and might therefore be exported from the TGN on the same carriers. In contrast, recycling transferrin receptors and the VSV-G protein traffic in distinct sets of tubules and vesicles devoid of GGA1.

The presence of both clathrin and GGA1 on the same carriers adds to the evidence that the GGAs function in association with clathrin (Puertollano *et al.*, 2001b; Costaguta *et al.*, 2001; Mullins and Bonifacino, 2001). The occurrence of AP-1 on these TGN-derived carriers, however, is intriguing

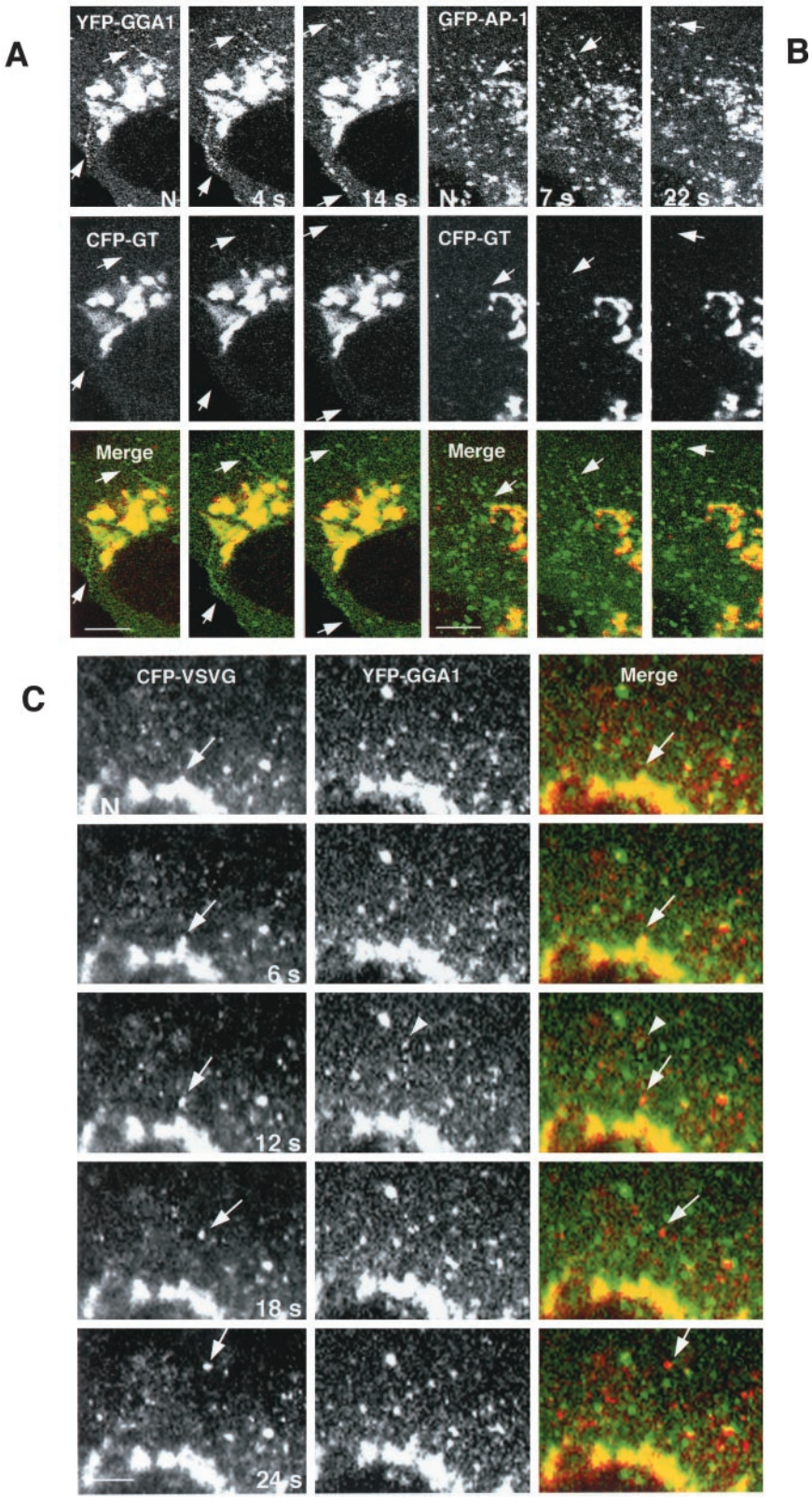

Figure 7. Exclusion of galactosyl transferase and VSV-G protein from GGA1 carriers budding from the TGN. (A and B) Golgi-resident protein galactosyl transferase (GT) is not incorporated into vesicular carriers budding from the TGN. MDCK cells were doubly transfected with a *trans*-Golgi resident protein (CFP-GT) and with YFP-GGA1 (A) or GFP-γ1 (GFP-AP-1) (B). Time-lapse microscopy showed the absence of CFP-GT (red channel) from rows of coated intermediates budding from the TGN (green channel, arrows). (C) VSV-G and GGA-1 localize to different transport intermediaries. MDCK cells, transfected with YFP-GGA1 and CFP-VSV-G (ts045 mutant) were incubated for 24 h at 40°C, shifted to 20°C for 1 h to accumulate cargo in the TGN, and then warmed to 32°C before visualization. Consecutive video images from time-lapse series show a VSV-G–enriched vesicle budding from the TGN (arrow, red channel). Note the absence of GGA1 (green channel) in this structure. The arrowhead points to a row of YFP-GGA1-containing vesicles rapidly budding from the TGN. N, nucleus. Bars, 10 μm (A and B), 5 μm (C).

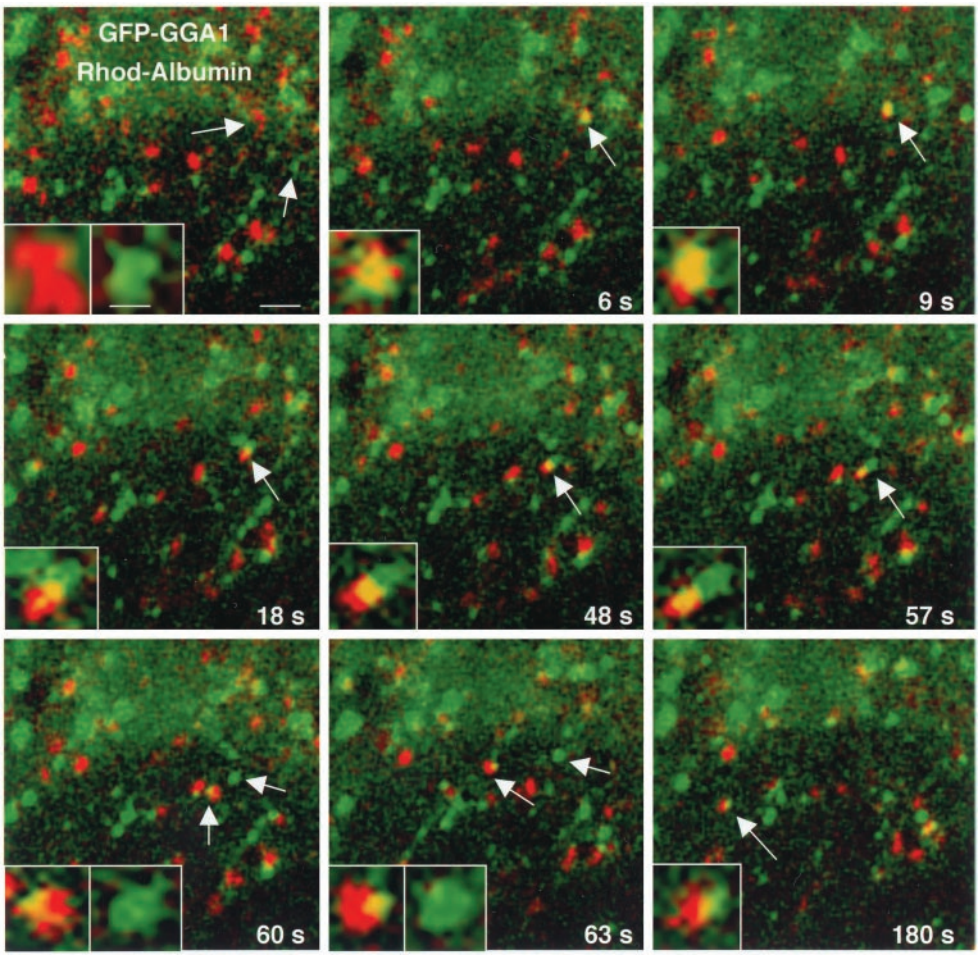

Figure 8. Interaction of GGA1-containing carriers with endosomes. MDCK cells were transfected with GFP-GGA1. At 15 h after transfection, the cells were loaded with rhodamine-albumin for 15 min before analysis by time-lapse confocal microscopy. Merged images for GFP-GGA1 (green) and rhodamine-albumin (red) are shown. Arrows point to vesicular structures containing rhodamine-albumin and GFP-GGA1. The insets show fourfold magnification of the structures pointed by the arrows. Bars, 2 and 0.5 μm (inset).

because the exact role of AP-1 in sorting is currently a matter of debate. Our observations with GFP-γ1-adaptin agree with those of Huang *et al.* (2001) obtained using YFP-μ1 to label the AP-1 complex. These authors reported that most YFP-μ1A–labeled vesicles also move from the TGN to the periphery of the cells. This sense of transport contrasts with the proposed role of AP-1 in recycling MPRs from endosomes to the TGN, inferred from the accumulation of MPRs in peripheral endosomes of μ1A-deficient fibroblasts (Meyer *et al.*, 2000). A possible explanation for these seemingly contradictory observations could be that AP-1 actually mediates removal of cargo from the intermediates as they move toward the cell periphery or upon their merge with peripheral endosomes. AP-1 has in fact been shown to function in the removal of membrane proteins from immature secretory granules after their budding from the TGN (Klumperman *et al.*, 1998). This would be analogous to the behavior of COPI, which is present on *v*esicular *t*ubular *c*lusters (VTCs) moving from endoplasmic reticulum (ER) exit sites to the Golgi complex (Presley *et al.*, 1997), even though it plays a role in protein recycling from the Golgi complex to the ER (Letourneur *et al.*, 1994). Another possibility is that AP-1 plays a role in sorting at the TGN, as previously assumed. Recent work suggests that the GGAs and AP-1 do cooperate to package MPRs into TGN-derived intermediates (Doray *et al.*, 2002b).

The TGN-derived coated intermediates described herein seem to belong to a growing family of large intracellular transport carriers, including VTCs, that mediate transport from the ER to the Golgi complex (Aridor *et al.*, 1995; Presley *et al.*, 1997) and PGCs involved in transport of VSV-G protein from the TGN to the plasma membrane (Hirschberg *et al.*, 1998; Polishchuk *et al.*, 2000). The large carriers described herein are the first ones shown to contain associated clathrin and GGA1. The decoration of tubules carrying the CD-MPR with GGA1 seem to occur in discontinuous manner, as if defining specific domains on the tubules. The CD-MPR was often more concentrated in the tubule domains containing associated GGA1, suggesting that the segregation of CD-MPR from other cargo molecules may persist after budding from the TGN.

The vesicular-tubular carriers containing CD-MPR and even the individual foci labeled for clathrin, GGA1, and AP-1 were apparently larger than plasma membrane-coated pits and conventional CCVs. This difference could be easily appreciated in microscopic fields where both types of clathrin-coated structures were visible (Figure 3D). Although the intensity of the fluorescence signal can impinge upon estimations of size by optical microscopy, in the case of clathrin it is reasonable to assume that the probability of GFP-labeled clathrin to be incorporated into clathrin lattices is the same

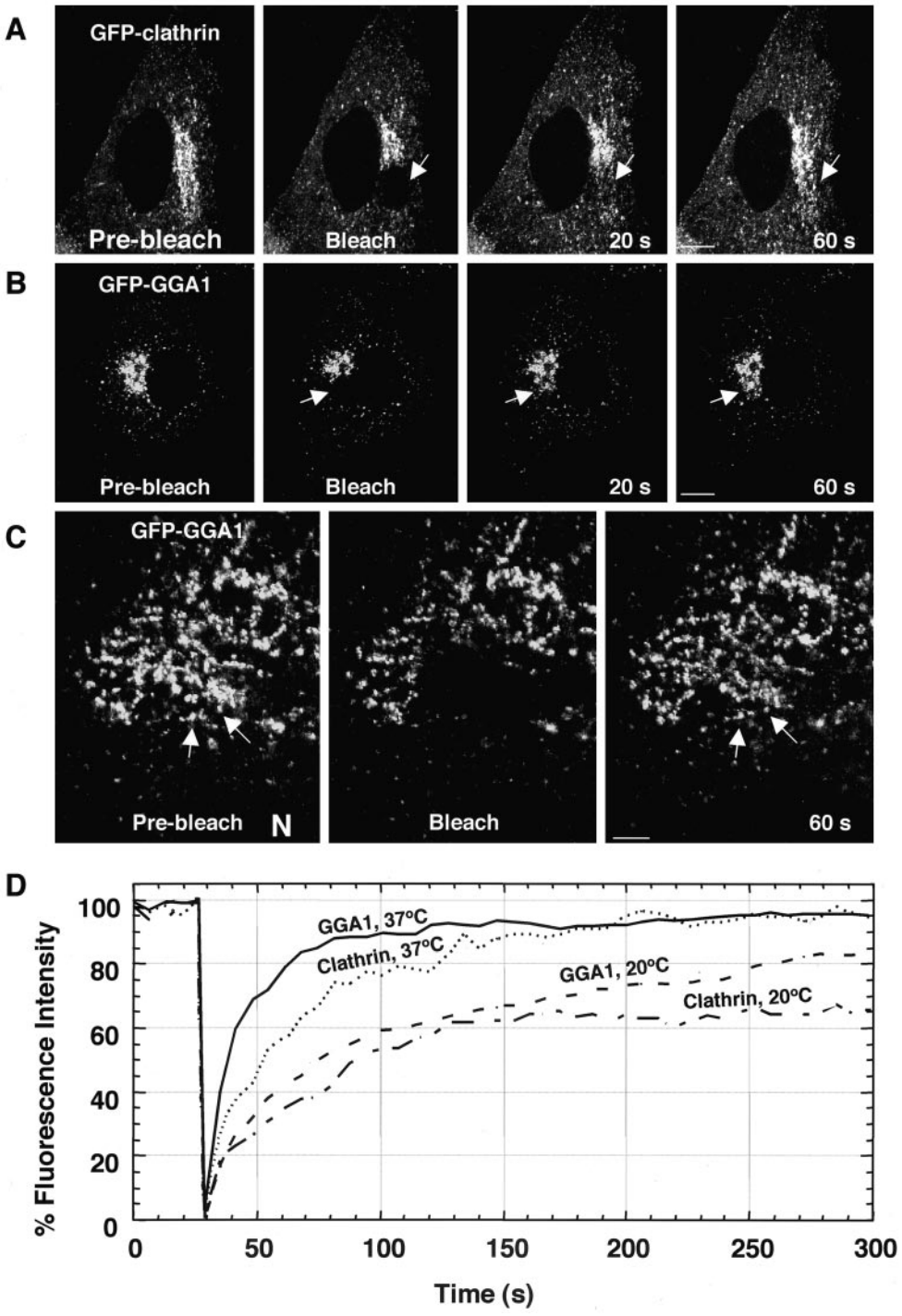

Figure 9. Dynamics of clathrin and GGA1 analyzed by fluorescence recovery after photobleaching. (A–C) MDCK cells were transiently transfected with constructs encoding GFP-clathrin (A) or GFP-GGA1 (B and C). Fluorescence associated with the Golgi complex was photobleached with high-intensity laser light and subsequent recovery of fluorescence was monitored by scanning the whole cell at low laser power at 5-s intervals for 5 min. The arrows in C indicate that the GFP-GGA1 recovers on the same TGN structures where it was located before photobleaching. N, nucleus. Bars, 10 μm (A and B), 5 μm (C). (D) Kinetics of GFP-clathrin and GFP-GGA1 recovery after photobleaching at 37 and 20°C. MDCK cells expressing GFP-clathrin or GFP-GGA1 were photobleached and then scanned at low laser power for 5 min. The graph shows the combined results of 10 determinations per condition. QuickTime videos of the experiments shown in panes A, B, and C can be seen in Supplemental Materials (videos A, B, and C).

in different parts of the cell. Thus, brighter clathrin-coated structures are also larger. Corroboration of the larger size of the TGN-derived intermediates was obtained by comparison with fluorescent beads of known size and similar brightness (Figure 4). The larger size of the TGN-intermediates was not due to "streaking" because the speed of scanning (typically 20–30 μm/s) was much higher than the speed of the intermediates (~1 μm/s).

The fine structure of the TGN-derived carriers could not be resolved by fluorescence microscopy because of limits on the resolution by this technique (~200 nm under the conditions of our experiments; Inoue, 1989). We envision that they

consist of tubular or irregularly shaped membrane-bound organelles (akin to VTCs [Aridor *et al.*, 1995] or PGCs [Polishchuk *et al.*, 2000]) with 60- to 130-nm coated buds that define specific domains within these organelles. The apparently larger size of the coated foci relative to CCVs could be due to the presence of several 60- to 130-nm coated buds on the carriers. It is also possible that the larger foci represent clusters of CCVs that are somehow tethered together.

An important property of the TGN-associated coats studied herein is that they are constantly cycling between membranes and the cytosol. Even when vesicle budding from the TGN is inhibited by incubation at 20°C, the coats continue to exchange. Therefore, dissociation of the coats does not require formation of vesicular intermediates. In this regard, the clathrin GGA– and AP-1–containing TGN coats behave like plasma membrane clathrin coats (Wu *et al.*, 2001) and COPI (Presley *et al.*, 2002), which also cycle on and off membranes when vesicle budding is inhibited. We were unable to examine the dynamics of coats on the TGN-derived intermediates themselves because of their mobility. In any event, whether dynamically or statically, the intermediates do retain their coats until they reach the periphery. The coats could thus be directly responsible for the recruitment of motor molecules that effect tracking along microtubules. The kinesin superfamily protein KIF13A, for example, is a plus-end microtubule motor that interacts with the β1-adaptin subunit of AP-1 (Nakagawa *et al.*, 2000). The coats could also bind tethering proteins that allow interactions or fusion of the intermediates with endosomes. For instance, rabaptin-5 is an effector of the early endosomal rab4 and rab5 GTP-binding proteins (Stenmark *et al.*, 1995; Vitale *et al.*, 1998) that also interacts with the γ1-adaptin subunit of AP-1 (Shiba *et al.*, 2002). The persistence of the coats on the intermediates may thus enable their involvement in organelle targeting events, in addition to their roles in vesicle formation and cargo selection.

Of course, our observations do not rule out the existence of small CCVs that could mediate short-range transfer of cargo to the larger intermediates or to endosomes located in the vicinity of the TGN. In fact, the endosomal recycling compartment (Yamashiro *et al.*, 1984) and late endosomes (Rabinowitz *et al.*, 1992) are mostly concentrated in the juxtanuclear area of the cell. It would be virtually impossible to observe direct transfer of materials from the TGN to these compartments. Small CCVs could also pinch off from the large intermediates as they move toward the peripheral cytoplasm. Finally, small CCVs could be too weakly labeled or transient for detection. Nevertheless, our findings do reveal the existence of a previously unrecognized type of intermediate containing associated clathrin coats, which could be involved in long-range delivery of biosynthetic cargo to peripheral cellular locations.

ACKNOWLEDGMENTS

We thank Jennifer Lippincott-Schwartz for helpful discussions and Margaret S. Robinson for kind gifts of reagents.

REFERENCES

Aridor, M., Bannykh, S.I., Rowe, T., and Balch, W.E. (1995). Sequential coupling between COPII and COPI vesicle coats in endoplasmic reticulum to Golgi transport. J. Cell Biol. *131*, 875–893.

Boman, A.L. (2001). GGA proteins: new players in the sorting game. J. Cell Sci. *114*, 3413–3418.

Brodsky, F.M., Chen, C.Y., Knuehl, C., Towler, M.C., and Wakeham, D.E. (2001). Biological basket weaving: formation and function of clathrin-coated vesicles. Annu. Rev. Cell Dev. Biol. *17*, 517–568.

Costaguta, G., Stefan, C.J., Bensen, E.S., Emr, S.D., and Payne, G.S. (2001). Yeast GGA coat proteins function with clathrin in Golgi to endosome transport. Mol. Biol. Cell *12*, 1885–96.

Damer, C.K., and O'Halloran, T.J. (2000). Spatially regulated recruitment of clathrin to the plasma membrane during capping and cell translocation. Mol. Biol. Cell *11*, 2151–2159.

Dell'Angelica, E.C., Puertollano, R., Mullins, C., Aguilar, R.C., Vargas, J.D., Hartnell, L.M., and Bonifacino, J.S. (2000). GGAs. A family of ADP ribosylation factor-binding proteins related to adaptors and associated with the Golgi complex. J. Cell Biol. *149*, 81–94.

Doray, B., Bruns, K., Ghosh, P., and Kornfeld, S. (2002a). Interaction of the cation-dependent mannose 6-phosphate receptor with GGA proteins. J. Biol. Chem. *277*, 18477–82.

Doray, B., Ghosh, P., Griffith, J., Geuze, H.J., and Kornfeld, S. (2002b). Cooperation of GGAs and AP-1 in packaging man-6-p receptors at the trans-Golgi network. Science *297*, 1700–1703.

Gaidarov, I., Santini, F., Warren, R.A., and Keen, J.H. (1999). Spatial control of coated-pit dynamics in living cells. Nat. Cell Biol. *1*, 1–7.

Griffiths, G., Pfeiffer, S., Simons, K., and Matlin, K. (1985). Exit of newly synthesized membrane proteins from the trans cisternae of the Golgi complex to the plasma membrane. J. Cell Biol. *101*, 949–964.

He, X., Chang, W.P., Koelsch, G., and Tang, J. (2002). Memapsin 2 (β-secretase) cytosolic domain binds to the VHS domains of GGA1 and GGA2: implications on the endocytosis mechanism of memapsin 2. FEBS Lett. *524*, 183–7.

Hirschberg, K., Miller, C.M., Ellenberg, J., Presley, J.F., Siggia, E.D., Phair, R.D., and Lippincott-Schwartz, J. (1998). Kinetic analysis of secretory protein traffic and characterization of Golgi to plasma membrane transport intermediates in living cells. J. Cell Biol. *143*, 1485–1503.

Hirst, J., Lindsay, M.R., and Robinson, M.S. (2001). GGAs. Roles of the different domains and comparison with AP-1 and clathrin. Mol. Biol. Cell *12*, 3573–3588.

Huang, F., Nesterov, A., Carter, R.E., and Sorkin, A. (2001). Trafficking of yellow-fluorescent-protein-tagged μ1 subunit of clathrin adaptor AP-1 complex in living cells. Traffic *2*, 345–357.

Inoue, S. (1989). Imaging of unresolved objects, superresolution, and precision of distance measurement with video microscopy. Methods Cell Biol. *30*, 85–112.

Jacobson, K., Derzko, Z., Wu, E.S., Hou, Y., and Poste, G. (1976). Measurement of the lateral mobility of cell surface components in single, living cells by fluorescence recovery after photobleaching. J. Supramol. Struct. *5*, 428.

Kirchhausen, T. (2000). Clathrin. Annu. Rev. Biochem. *69*, 699–727.

Klumperman, J., Kuliawat, R., Griffith, J.M., Geuze, H.J., and Arvan, P. (1998). Mannose 6-phosphate receptors are sorted from immature secretory granules via adaptor protein AP-1, clathrin, and syntaxin 6-positive vesicles. J. Cell Biol. *141*, 359–371.

Letourneur, F., Gaynor, E.C., Hennecke, S., Demolliere, C., Duden, R., Emr, S.D., Riezman, H., and Cosson, P. (1994). Coatomer is essential for retrieval of dilysine-tagged proteins to the endoplasmic reticulum. Cell *79*, 1199–1207.

Meyer, C., Zizioli, D., Lausmann, S., Eskelinen, E.L., Hamann, J., Saftig, P., von Figura, K., and Schu, P. (2000). μ1a-Adaptin-deficient

mice: lethality, loss of AP-1 binding and rerouting of mannose 6-phosphate receptors. EMBO J. *19*, 2193–2203.

Mullins, C., and Bonifacino, J.S. (2001). Structural requirements for function of yeast GGAs in vacuolar protein sorting, α-factor maturation, and interactions with clathrin. Mol. Cell. Biol. *21*, 7981–7994.

Nakagawa, T., Setou, M., Seog, D., Ogasawara, K., Dohmae, N., Takio, K., and Hirokawa, N. (2000). A novel motor, kif13a, transports mannose-6-phosphate receptor to plasma membrane through direct interaction with AP-1 complex. Cell *103*, 569–581.

Nielsen, M.S., Madsen, P., Christensen, E.I., Nykjaer, A., Gliemann, J., Kasper, D., Pohlmann, R., and Petersen, C.M. (2001). The sortilin cytoplasmic tail conveys Golgi-endosome transport and binds the VHS domain of the GGA2 sorting protein. EMBO J. *20*, 2180–2190.

Nishimura, Y., Kawabata, T., Yano, S., and Kato, K. (1990). Inhibition of intracellular sorting and processing of lysosomal cathepsins h and l at reduced temperature in primary cultures of rat hepatocytes. Arch. Biochem. Biophys. *283*, 458–463.

Peters, P.J. (1998). Cryo-immunogold electron microscopy. In: Current Protocols in Cell Biology, ed. J.S. Bonifacino, M. Dasso, J.B. Harford, J. Lippincott-Schwartz, and K. Yamada, New York: John Wiley & Sons, 4.7.1–4.7.12.

Polishchuk, R.S., Polishchuk, E.V., Marra, P., Alberti, S., Buccione, R., Luini, A., and Mironov, A.A. (2000). Correlative light-electron microscopy reveals the tubular-saccular ultrastructure of carriers operating between Golgi apparatus and plasma membrane. J. Cell Biol. *148*, 45–58.

Porcelli, S., Morita, C.T., and Brenner, M.B. (1992). Cd1b restricts the response of human CD4-8-t lymphocytes to a microbial antigen. Nature *360*, 593–597.

Presley, J.F., Cole, N.B., Schroer, T.A., Hirschberg, K., Zaal, K.J., and Lippincott-Schwartz, J. (1997). ER-to-Golgi transport visualized in living cells. Nature *389*, 81–85.

Presley, J.F., Ward, T.H., Pfeiffer, A., Siggia, E.D., Phair, R.D., and Lippincott-Schwartz, J. (2002). Dissection of copi and arf1 dynamics in vivo and role in Golgi membrane transport. Nature *417*, 187–193.

Puertollano, R., Aguilar, R.C., Gorshkova, I., Crouch, R.J., and Bonifacino, J.S. (2001a). Sorting of mannose 6-phosphate receptors mediated by the GGAs. Science *292*, 1712–1716.

Puertollano, R., Randazzo, P., Hartnell, L.M., Presley, J., and Bonifacino, J.S. (2001b). The GGAs promote ARF-dependent recruitment of clathrin to the TGN. Cell *105*, 93–102.

Rabinowitz, S., Horstmann, H., Gordon, S., and Griffiths, G. (1992). Immunocytochemical characterization of the endocytic and phagolysosomal compartments in peritoneal macrophages. J. Cell Biol. *116*, 95–112.

Robinson, M.S., and Bonifacino, J.S. (2001). Adaptor-related proteins. Curr. Opin. Cell Biol. *13*, 444–453.

Shiba, Y., Takatsu, H., Shin, H.W., and Nakayama, K. (2002). γ-Adaptin interacts directly with rabaptin-5 through its ear domain. J. Biochem. *131*, 327–336.

Stenmark, H., Vitale, G., Ullrich, O., and Zerial, M. (1995). Rabaptin-5 is a direct effector of the small GTPase rab5 in endocytic membrane fusion. Cell *83*, 423–432.

Storrie, B., and Desjardins, M. (1996). The biogenesis of lysosomes: is it a kiss and run, continuous fusion and fission process? Bioessays *18*, 895–903.

Takatsu, H., Katoh, Y., Shiba, Y., and Nakayama, K. (2001). Golgi-localizing, γ-adaptin ear homology domain, ADP-ribosylation factor-binding (GGA) proteins interact with acidic dileucine sequences within the cytoplasmic domains of sorting receptors through their vps27p/hrs/stam (VHS) domains. J. Biol. Chem. *276*, 28541–28545.

Vitale, G., Rybin, V., Christoforidis, S., Thornqvist, P., McCaffrey, M., Stenmark, H., and Zerial, M. (1998). Distinct rab-binding domains mediate the interaction of rabaptin-5 with GTP-bound rab4 and rab5. EMBO J. *17*, 1941–1951.

Wacker, I., Kaether, C., Kromer, A., Migala, A., Almers, W., and Gerdes, H.H. (1997). Microtubule-dependent transport of secretory vesicles visualized in real time with a GFP-tagged secretory protein. J. Cell Sci. *110*, 1453–63.

Wu, X., Zhao, X., Baylor, L., Kaushal, S., Eisenberg, E., and Greene, L.E. (2001). Clathrin exchange during clathrin-mediated endocytosis. J. Cell Biol. *155*, 291–300.

Xu, H., and Shields, D. (1993). Prohormone processing in the trans-Golgi network: endoproteolytic cleavage of prosomatostatin and formation of nascent secretory vesicles in permeabilized cells. J. Cell Biol. *122*, 1169–1184.

Yamashiro, D.J., Tycko, B., Fluss, S.R., and Maxfield, F.R. (1984). Segregation of transferrin to a mildly acidic (ph 6.5) para-Golgi compartment in the recycling pathway. Cell *37*, 789–800.

Zhu, Y., Doray, B., Poussu, A., Lehto, V.P., and Kornfeld, S. (2001). Binding of GGA2 to the lysosomal enzyme sorting motif of the mannose 6-phosphate receptor. Science *292*, 1716–1718.